and are at best rough estimates; nor, for that matter, do the experimental surfaces measure up to the smooth statistical distribution assumed in the theory.

In spite of the acknowledged shortcomings, we feel that the experiments provide the first explicit evidence for increasingly diffuse scattering with increasing angle of incidence to the surface for a specific group of electrons at the Fermi surface. The experiments also hold the promise of even more detailed quantitative information on diffuse scattering. Our results substantiate and make appear reasonable theoretical discussions of an angle-dependent specularity parameter as in the work of Greene and O'Donnell[12] and of Soffer.[13]

ACKNOWLEDGMENTS

We acknowledge the many useful discussions regarding surface scattering with R. F. Greene, S. P. Singhal, and R. E. Prange. We also thank C. C. Kuo, J. R. Maldonado, and K. Sibbald for participating in some phases of the experimental work.

[12] R. F. Greene and R. W. O'Donnell, Phys. Rev. **147**, 599 (1966).
[13] S. B. Soffer, Bull. Am. Phys. Soc. **14**, 594 (1969).

PHYSICAL REVIEW VOLUME 186, NUMBER 3 15 OCTOBER 1969

Bulk Current Instabilities in Uniaxially Strained Germanium

JOHN E. SMITH, JR., JAMES C. MCGRODDY, AND MARSHALL I. NATHAN
IBM Watson Research Center, Yorktown Heights, New York 10598
(Received 14 April 1969)

Experimental studies of current instabilities in uniaxially compressed *n*- and *p*-type germanium are described. The instability reflects the presence of bulk negative differential conductivity due to transfer of carriers between the strain-split high-mobility and low-mobility states of the conduction or valence band. At low temperatures, threshold fields of the order of several hundred volts per centimeter are observed, which is an order of magnitude smaller than the threshold electric field for the Gunn effect in GaAs. In *n*-type Ge, the effect is observed at room temperature. The dependence of these phenomena on temperature, sample orientation, and stress magnitude is discussed. These results demonstrate the importance of intervalley transfer to the X minima in determining the high-field transport properties of *n*-type Ge. Unsuccessful attempts to observe similar effects in strained *p*-type InSb and *n*-type Si are also described and discussed.

I. INTRODUCTION

IN semiconducting materials where the current is carried by electrons or holes in a degenerate conduction or valence band, removal of these degeneracies by the application of uniaxial stress can result in gross changes in the electrical conductivity. The consequent large piezoresistance coefficients have been used to determine the symmetry of conduction and valence bands for a large number of materials. In addition to these effects on the low-field conductivity, the removal of band degeneracies markedly affects the dependance of carrier velocities on applied electric field in the non-ohmic "warm" and "hot" electron regions.

Ridley and Watkins[1] and Hilsum[2] considered the possibility of realizing bulk negative differential conductivity (BNDC) due to intervalley transfer of carriers in semiconductors with multivalley conduction-band structure. Although the primary emphasis in the study of BNDC effects has been on the study of the Gunn effect in *n*-type GaAs,[3] BNDC and resulting current instabilities have recently been reported in both *p*-type[4] and *n*-type[5] Ge under conditions of appropriately oriented uniaxial compression and electric field. The earlier work on *p*-type Ge was confined to temperatures near 4.2°K, while *n*-type materials have been studied between 27°K and room temperature. The present paper is a report of an extension of these previous studies. In *n*-type Ge the phenomenon has been studied in a wide variety of orientations as a function of temperature and magnitude of applied stress. Studies on *p*-type Ge as a function of stress were carried out at higher temperatures than the original studies, namely, from 27 to 160°K. (The effect has not been observed above 160°K in *p*-type Ge.) In addition, we report on some unsuccessful attempts to observe similar phenomena in *n*-type Si and *p*-type InSb.

In Sec. II, we discuss sample preparation and other experimental details. Section III contains a discussion

[1] B. K. Ridley and T. B. Watkins, Proc. Phys. Soc. (London) **78**, 293 (1961).
[2] C. Hilsum, Proc. IRE **50**, 185 (1962).
[3] J. B. Gunn, Solid State Commun. **1**, 89 (1963); IBM J. Res. Develop. **8**, 141 (1964); subsequent work is reviewed in P. N. Butcher, Rept. Progr. Phys. **30**, 97 (1967).
[4] A. A. Kastal'skii and S. M. Ryvkin, Fiz. Tech. Poluprov. **1**, 622 (1967) [English transl.: Soviet Phys.—Semicond. **1**, 523 (1967)].
[5] J. E. Smith, Jr., Appl. Phys. Letters **12**, 233 (1968).

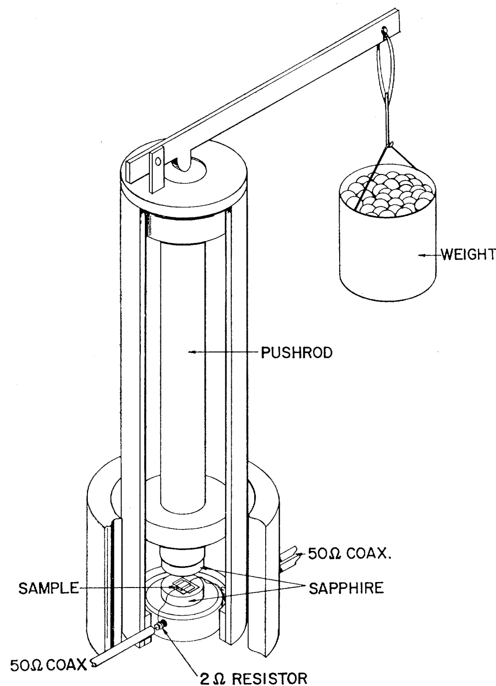

FIG. 1. Schematic drawing of uniaxial stress apparatus. For measurements at 77 or 27°K, the lower part of the apparatus is immersed in liquid nitrogen or neon, respectively.

of the effects of stress on n-type Ge as well as the experimental results for that material, and a similar discussion for n-type Si. Finally, results for p-type Ge and p-type InSb are presented and discussed.

II. EXPERIMENTAL PROCEDURE

The samples were rectangular parallelepipeds with typical edge dimensions of 0.5–1 mm. In order to prepare the samples, oriented wafers were cut from single-crystal ingots using a diamond saw. The wafers were lapped to the desired sample length and polished on both sides. Ohmic contacts were then formed on both faces of the wafers using several techniques. For the n-type Ge samples, the contacts were formed by diffusion of As at 700°C for 24 h. For the p-type Ge samples, the ohmic contacts were formed either by diffusion of Ga through a thin layer of SiO_2, which ensured that the resulting surfaces were undamaged, or by bombarding the surface with 240-keV B^{11} ions, the total doses being 1×10^{15} cm^{-2}. No heat treatment was required for the implanted contacts—in fact, the ohmic nature of the contacts may have been due not to the acceptor character of B, but to the fact that thin layers of polycrystalline or disordered Ge is heavily p-type.[6] The contacts to n-type Si were formed by diffusion of P. The p-type InSb was contacted by diffusing with Zn. After the ohmic contacts were formed, the wafers were electroplated with Au, electrolessly plated with Ni, and again plated with Au. The contacted wafers were again x-ray oriented and bars were cut from the wafers with a diamond saw. The sawed surfaces were lapped to the desired dimensions and polished. Sufficient material was removed in the lapping process to eliminate the effect of damage from the diamond saw. The final cuts were made with a wire saw using a 3.5-mil blade and a 5-μ grit. For the cases where stress was to be applied perpendicular to the current direction, wires were attached to the contact faces of the samples using low-melting-point solder. The longitudinally stressed samples were mounted in stress apparatus with 1-mil brass shim stock making contact to the contact faces. The current pulses resulting when flat-topped voltage pulses were applied to the sample were also flat-topped, indicating that the contacts were in fact noninjecting.

The apparatus used to apply the stress is shown schematically in Fig. 1. It has been briefly described previously and is extremely simple. The sample is mounted on one of a pair of sapphire disks, which in turn is mounted in a sample holder designed with adequate electrical characteristics for the short pulse used. The sample holder fits into a jig which contains a push rod, on the end of which is mounted the other parallel sapphire disk. If the sample is to be stressed longitudinally, the brass shim leaves are mounted on the two sapphires to provide electrical contact; in the transverse stress configuration pieces of 0.0006-cm Mylar are placed between the sample and the sapphire disks to improve the uniformity of the applied stress. The fracture stress for samples mounted in this way is typically 1.5×10^4 kg/cm^2 at 77°K, corresponding to a fractional linear compression of approximately 1.5%.

The pulses, usually 20 nsec long, were supplied by a discharge line pulse generator connected to the sample by 50-Ω coaxial cables. The voltage and current were measured using a two-channel Tektronix 661 oscilloscope with either a 4S1 or 4S2 sampling amplifier. A 2-Ω shunt resistor was used to monitor the current. The output of the oscilloscope was connected to an xy recorder which could be used to plot either the sample current-voltage curve at a fixed time relative to the onset of the voltage pulse, or current or voltage waveforms as a function of time.

A typical set of current-voltage characteristics for various values of applied stress is shown in Fig. 2. For stresses large enough to produce the BNDC effect, the curves in Fig. 2 terminate at the threshold voltage. The threshold voltage is determined in the following manner: If the BNDC effect is sufficiently large, and the sampling time is chosen to be about half the electron transit time across the sample, exceeding the threshold causes the formation of a high-field travelling domain, which reduces the current in the sample during the transit. The resulting decrease in current

[6] J. E. Davey, R. J. Tierman, T. Pankey, and M. D. Montgomery, Solid State Electron. 6, 205 (1963).

when threshold is reached is obvious. For cases where the BNDC effect is weaker, the current oscillations are smaller in amplitude and strong dependence of the oscillation frequency on applied voltage produces clearly identifiable structure on the current-voltage characteristic, which again unambiguously identifies the threshold voltage. In the absence of detailed measurements of the electric field distribution in the samples, the threshold electric field is taken to be the average field, the threshold voltage divided by the sample length, corrected for the length of the heavily doped contact regions.

The data reported in this paper is taken from samples whose behavior was independent of polarity—that is, at a given value of stress, the threshold fields for the two polarities of applied voltage differed by less than 5% of their mean and the current-voltage characteristics were independent of polarity below threshold. For cases where the BNDC effect is relatively weak and well-formed Gunn domains are not formed (as indicated by the current waveform), the above procedure may be less reliable, since the field in the sample is not uniform.

The stresses quoted throughout this paper are stresses assuming uniform strain. It is likely that the samples are distorted somewhat due to partial clamping of the sides of the samples to which force is applied, and that the resulting strain distribution is nonuniform. (The samples were typically shaped so that the cross section normal to the current direction was square, and the electrical length was approximately 1.5 times the length of a side of this square.) Without knowing in detail the degree of clamping of the sides of the samples, it is impossible to give a quantitative estimate of the degree of nonuniformity of the strain. There is nothing in our experimental results to suggest that this is an important effect, and indeed the high fracture stresses observed suggest good uniformity. However, the energy splitting of the valleys discussed in the next section probably varies somewhat over the length of the sample.

III. RESULTS AND DISCUSSION

A. n-Type Germanium

Since the conduction-band minima in Ge lie along $\langle 111\rangle$ directions in k space, the degeneracy of these minima is lifted only by shear strain components—i.e., the splitting involves only the elastic compliance S_{44}. For a uniform uniaxial compression of magnitude x applied to a plane normal to

$$\mathbf{d}=d_1\mathbf{u}_1+d_2\mathbf{u}_2+d_3\mathbf{u}_3\,, \tag{1}$$

where the $\mathbf{u}_1$, $\mathbf{u}_2$, and $\mathbf{u}_3$ are unit vectors along the cubic-crystal axes, the stress tensor is given by

$$\mathbf{X}=x\begin{bmatrix} d_1^2 & d_1d_2 & d_1d_3 \\ d_1d_2 & d_2^2 & d_2d_3 \\ d_1d_3 & d_2d_3 & d_3^2 \end{bmatrix}. \tag{2}$$

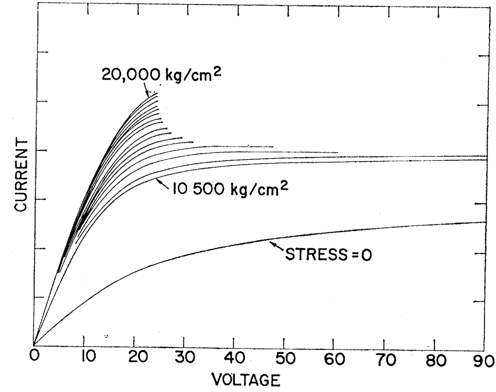

FIG. 2. Typical current-voltage characteristics for a sample of p-type Ge. The upper ends of the I-V curves represent the threshold for current oscillations; above the threshold the I-V characteristic depends on the sampling time chosen, and is not shown here.

If we use the deformation potential

$$\mathbf{\Xi}^\nu=\Xi_d{}^\nu\mathbf{1}+\Xi_u i_i{}^\nu i_j{}^\nu\mathbf{u}_i\mathbf{u}_j\,, \tag{3}$$

where $\mathbf{i}^\nu=i_1{}^\nu\mathbf{u}_1+i_2{}^\nu\mathbf{u}_2+i_3{}^\nu\mathbf{u}_3$ is a unit vector parallel to the axis of revolution of the conduction-band valley identified by the index ν and $\mathbf{1}$ is the unit dyadic, and retaining only the terms which split the degeneracy, the relative shifts of the valley minima with stress are given by

$$\delta\epsilon_\nu=(\Xi_u S_{44}x)(i_1{}^\nu i_2{}^\nu d_1d_2+i_1{}^\nu i_3{}^\nu d_1d_3+i_2{}^\nu i_3{}^\nu d_2d_3)\,. \tag{4}$$

The constant Ξ_u has the value 15.8 eV,[7] and S_{44} was taken as 1.457×10^{-6} cm²/kg.

In all the experiments reported here the direction along which the uniaxial compression was applied lies in a $\{110\}$ plane. For that case the expression for the splitting can be written as

$$\delta\epsilon_\nu=S_{44}x\Xi_u[(i_1{}^\nu i_2{}^\nu+i_1{}^\nu i_3{}^\nu)(\cos\alpha\sin\alpha/\sqrt{2}) +\tfrac{1}{2}i_2{}^\nu i_3{}^\nu\sin^2\alpha]\,, \tag{5}$$

where α is the angle between the direction of uniaxial compression [lying in the $(01\bar{1})$ plane] and the [100] direction. The relative energies of the four $\langle 111\rangle$ valley minima are plotted as a function of α for fixed x in Fig. 3.

The constant-energy surfaces near these minima are prolate ellipsoids having a large effective-mass anisotropy, the longitudinal mass being 19.07 times larger than the transverse mass.[8] This fact, combined with a knowledge of the splitting discussed above, enables one to readily find relative orientations of uniaxial compression and current flow which are qualitatively favorable for the observation of a BNDC effect. The orientations in which we have observed current oscillations due to BNDC in n-type Ge are listed in Table I.

[7] J. J. Hall (private communication).
[8] B. W. Levinger and D. R. Frankl, J. Phys. Chem. Solids **20**, 281 (1961).

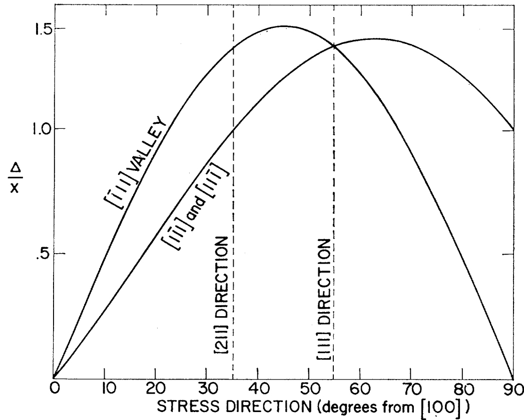

FIG. 3. Relative valley-edge position (in energy) as a function of stress direction. The directions plotted are in the (011̄) plane; 0 is [100] and 90° is [011]. Δ/X is in arbitrary units.

We first discuss in detail the results for the case where the uniaxial compression is along a ⟨111⟩ direction. This choice of stress direction maximizes the energy splitting of the valleys for a given stress; the valley lying along the stress direction is lowered in energy relative to the other three, which remain degenerate. The current direction must be either parallel or perpendicular to the stress direction, so that in this case, in order to produce BNDC by intervalley transfer, the current must be in a {111} plane. If we define the conductivity effective mass m_c by

$$1/m_c = \mathbf{u}\cdot(1/\mathbf{m}^*)^\nu\cdot\mathbf{u}, \tag{6}$$

where $\mathbf{u}$ is a unit vector in the current direction and $(1/\mathbf{m}^*)^\nu$ is the inverse effective-mass tensor for the valley designated by the index ν. The dependence of m_c on current direction in the (111) plane is shown in Fig. 4. The [2̄11] current direction provides the maximum effective mass for one of the higher-lying valleys, and has been studied in greatest detail. BNDC and current oscillations have been observed for the [1̄10] current direction with [111] stress, but the effects are weaker. No detailed measurements have been made in this configuration.

TABLE I. Conductivity effective masses and valley edge splittings for the ⟨111⟩ conduction-band valleys in strained Ge. The configurations of stress and current directions in which current instabilities occur in n-type Ge are listed.

	Current direction	Stress direction	Splitting[a]	m_e/m_t	Masses[b] m_i/m_t	m_h/m_t
A	[211]	[1̄11]	0.102	1.00(1)	— (0)	1.27(2) 6.44(1)
B	[211]	[011̄]	0.076	1.27(2)	— (0)	1.00(1) 6.44(1)
C	[111]	[2̄11]	0.102	1.11(1)	1.11(2)	19.07(1)
D	[111]	[011̄]	0.076	1.11(2)	— (0)	1.11(1) 19.07(1)
E	[421]	[1̄12]	0.102	1.02(1)	1.68(1) 3.79(1)	1.12(1)
F	[110]	[1̄10]	0.076	1.00(2)	— (0)	2.72(2)
G	[110]	[1̄11]	0.102	1.00(1)	— (0)	1.00(1) 2.72(2)

[a] The splitting indicated is that between the lowest valley or valleys and the next lowest for a stress of 10 000 kg/cm².
[b] m_e is the conductivity effective mass of electrons in the valley(s) lying lowest in energy, m_i intermediate in energy, and m_h highest. m_t is the transverse mass; we take $K=19.07$.

Figure 5 shows the dependence of the threshold field on applied stress for the case of [111] compression and [2̄11] current at three temperatures: 27, 77°K, and room temperature. A rather striking feature of all these curves, and one which we find to be the rule rather than the exception, is that upon increasing the stress above the minimum required to produce BNDC, the threshold voltage at first decreases with increasing stress, and finally increases with increasing stress. This nonintuitive feature of the experimental results is discussed in more detail below. As would be expected intuitively, the characteristic stresses and fields, i.e., the minimum stress necessary to produce BNDC, as well as the minimum threshold field and the stress associated with this threshold field, all increase with increasing lattice temperature. While the details of the experimental results, such as shown in Fig. 5, varied somewhat from one crystal to another, no systematic dependence of the results on carrier concentration was observed except avalanche breakdown was observed in the more heavily doped samples. The carrier concentration of the samples studied ranged from 9×10^{13} cm^{-3} to 1.8×10^{16} cm^{-3} (room-temperature resistivity 0.13–17 Ω cm).

An obvious alternate procedure for the choice of current and stress directions is to choose the current to be in a ⟨111⟩ direction, so that electrons in the valley lying along that direction will have the full longitudinal effective mass. Then compression applied along directions in the plane normal to the current direction will result in situations favorable for the observation of BNDC due to intervalley transfer. We have studied the cases where the stress is in the ⟨211⟩

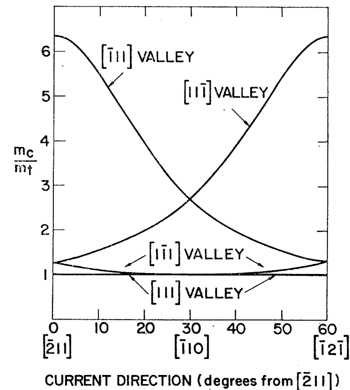

FIG. 4. Conductivity effective mass versus current direction for the four ⟨111⟩ valleys of Ge, assuming the mass anisotropy to be given by $K=19.07$.

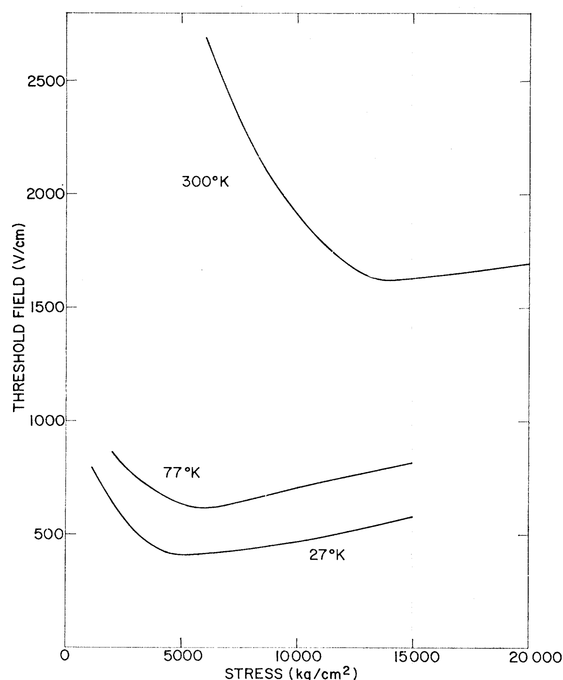

FIG. 5. Threshold field versus uniaxial stress for n-type Ge with room-temperature resistivity $\rho=1\ \Omega$ cm and $n=1.9\times10^{15}$ cm^{-3}. Stress is in the [111] direction and current in the [$\bar{2}$11] direction. The temperatures for the three curves are 27, 77, and 300°K, as shown on the figure.

and ⟨110⟩ directions in this plane. The dependence of threshold field on stress for both configurations is given in Fig. 6 (27°K) and Fig. 7. (77°K). The effect has also been observed at room temperature for the ⟨211⟩ stress case, but the oscillations have been smaller in amplitude and less reproducible than those observed in the [$\bar{2}$11] current, [111] stress configuration described earlier.

Instabilities have also been observed at 27 and 77°K for configurations with [124] current and [21$\bar{1}$] stress, [211] current and [01$\bar{1}$] stress, [110] current and both [$\bar{1}$11] and [$\bar{1}$10] stress. The last situation, [110] current and [$\bar{1}$10] stress, results in a particularly simple valley configuration: The four valleys are split into two groups of two, the lower valleys having the minimum possible effective mass, namely, the transverse effective mass (m_t), while in the upper valleys the effective mass is $2.7m_t$. This results in threshold fields somewhat higher than situations with just one lowest-energy valley.

Situations where the current is in a ⟨110⟩ direction, for example, the situation depicted by the threshold field-stress curve F in Fig. 6, are peculiar in that the current instability is observed at zero stress. This is the instability reported by McGroddy and Nathan.[9] In the ⟨110⟩ direction, it is generally very much weaker than in the ⟨100⟩ direction, and has higher threshold field. As seen in Fig. 6, curve C, the threshold field decreases rapidly by a factor of more than 2, since the ⟨111⟩ valleys are split by the strain, and intervalley transfer between these valleys begins to contribute to the BNDC. At the same time, we find a dramatic increase in the amplitude of the associated current oscillations.

In summary, in every configuration which qualitatively seems suitable for the production of a BNDC effect in strained n-type Ge, such an effect has been observed at 27 and 77°K. However, the effect is generally weaker at the higher temperature, and at room temperature, it is observed only in the configurations of [111] stress, [$\bar{2}$11] current and [$\bar{2}$11] stress, [111] current. At all temperatures, the threshold fields have been lowest and amplitudes of the current oscillations greatest in the [111] stress, [$\bar{2}$11] current configuration.

Without exception the measured threshold-field-versus-stress curves exhibit a minimum as the stress is increased above the minimum required to depopulate the upper minima at equilibrium. This fact indicates that in the absence of a detailed understanding of the dynamics of an intervalley-transfer type of BNDC effect in a particular case, extreme caution must be used in interpreting the results of the dependence of threshold fields on stress, pressure, or alloy compositions.

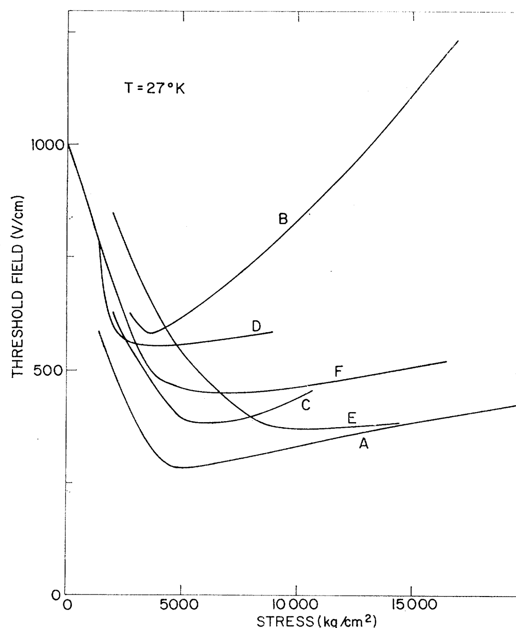

FIG. 6. Threshold field versus uniaxial stress for a variety of configurations at 27°K. Current directions, stress directions, and room-temperature resistivities (in Ω cm) for the various curves are (A) [211], [$\bar{1}$11], 6.3; (B) [211], [01$\bar{1}$], 6.3; (C) [111], [$\bar{2}$11], 6.3; (D) [111], [01$\bar{1}$], 6.3; (E) [421], [$\bar{1}$12], 2; (F) [110], [$\bar{1}$10], 2; and (G) [110], [$\bar{1}$11], 6.3. Curve B ends at its intersection with curve C. Same designations of configurations as in Table I.

[9] J. C. McGroddy and M. I. Nathan, IBM J. Res. Develop. **11**, 337 (1967).

TABLE II. Relative effective masses for uniaxially strained p-type Ge and InSb. The splitting for ⟨111⟩ stress is given by $S_{44}dX/\sqrt{3}$ and for ⟨100⟩ by $2(S_{11}-S_{12})\,bX$. The subscripts $\parallel$ and $\perp$ on the effective masses refer to current parallel to and normal to the stress direction; $m(1)$ is the effective mass of the higher electron-energy subband and $m(2)$, the lower.

Stress direction	p-type Ge[a]		p-type InSb[b]	
⟨111⟩	$m_{\parallel}^{-1}(1)=23.6$	$m_{\parallel}^{-1}(2)=2.4$	$m_{\parallel}^{-1}(1)=63.4$	$m_{\parallel}^{-1}(2)=1.6$
	$m_{\perp}^{-1}(1)=7.7$	$m_{\perp}^{-1}(2)=18.3$	$m_{\perp}^{-1}(1)=17.0$	$m_{\perp}^{-1}(2)=48.0$
⟨100⟩	$m_{\parallel}^{-1}(1)=21.9$	$m_{\parallel}^{-1}(2)=4.1$	$m_{\parallel}^{-1}(1)=61.1$	$m_{\parallel}^{-1}(2)=3.9$
	$m_{\perp}^{-1}(1)=8.55$	$m_{\perp}^{-1}(2)=17.5$	$m_{\perp}^{-1}(1)=18.2$	$m_{\perp}^{-1}(2)=46.8$

[a] Reference 14. [b] C. R. Pidgeon and R. N. Brown, Phys. Rev. **146**, 575 (1966).

The existence of this type of dependence of threshold field on energy separation between the relevant sets of minima can be understood qualitatively as a consequence of the sublinear dependence of electron drift velocity on electric field for a single minimum. In the simplest model, we have two minima having electron concentrations n_L in the lower-energy high-mobility minimum, and $n_u=n_0-n_l$ in the higher-energy low-mobility minimum, where n_0 is the field-independent carrier concentration. The field-dependent drift velocities in these minima are $V_l(E)$ and $V_u(E)$, respectively. Then, the average drift velocity is

$$V(E)=\{n_l(E)V_l(E)+[n_0-n_l(E)]V_u(E)\}/n_0, \quad (7)$$

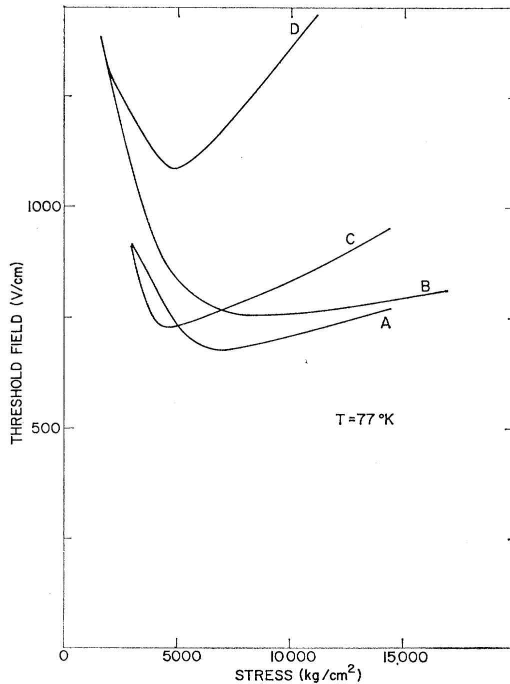

FIG. 7. Threshold field versus stress for a variety of configurations at 77°K. Current directions, stress directions, and room-temperature resistivities (in Ω cm) of the material for the various curves are (A) [211], [$\bar{1}$11], 2; (B) [211], [01$\bar{1}$], 6.3; (C) [111], [$\bar{2}$11], 6.3; and (D) [111], [01$\bar{1}$], 2. Curve C ends at its intersection with curve A. These configurations are labeled with the same letters in Fig. 6 and Fig. 7 as well as Table I, but not necessarily the same samples.

and the threshold field is determined from

$$n_0\frac{dV(E)}{dE}=0=[V_l(E)-V_u(E)]\frac{dn_l(E)}{dE}+n_l(E)\frac{dV_l(E)}{dE}+[n_0-n_l(E)]\frac{dV_u(E)}{dE}. \quad (8)$$

The first term is negative, while the last two terms as well as the second factor of the first term are positive.

For many scattering mechanisms, $V_l(E)$ and $V_u(E)$ will be less than linear in E at high electric fields. Consider the case where $V_l(E)$ and $V_u(E)$ tend to saturate. If the energy separation Δ between the lower and upper valleys is small, most of the transfer will occur at small values of E, where the last two terms of Eq. (8) are larger, and where the first factor of the first term is small, preventing the occurrence of BNDC in this range of electric fields. However, as soon as Δ is large enough to permit dn_l/dE to remain finite at fields where $V_l(E)$ and $V_u(E)$ tend to saturate, BNDC can occur, and the threshold field will be in the range of fields where the velocities saturate. At somewhat larger values of Δ, the transfer will not occur at all at very small fields, but will be large enough in a range of fields below velocity saturation, where the first factor of the first term is quite large, and the threshold field will be less than that required to produce saturation in the individual valleys. Finally, at very high values of Δ, the threshold field must again rise, since a larger field is required to produce any substantial transfer. A simple model which incorporates this nonohmic behavior in the individual valleys gives a semiquantitative explanation of the observed dependence of threshold field on stress.[10]

B. Relation to the BNDC in Unstrained n-Type Ge

The data discussed above shed some light on the origin of the BNDC effect observed in n-type Ge below about 120°K,[11] in particular providing an estimate of

[10] J. E. Smith, Jr., J. C. McGroddy, and M. I. Nathan, in *Proceedings of the Ninth International Conference on the Physics of Semiconductors*, edited by S. M. Ryvkin (Nauka Publishing House, Leningrad, 1969), p. 950.

[11] B. J. Elliott, J. B. Gunn, and J. C. McGroddy, Appl. Phys. Letters **11**, 253 (1967).

the importance of transfer to the ⟨100⟩ siliconlike minima, which are located approximately 0.18 eV above the normally occupied ⟨111⟩ minima.[12] At 77°K the threshold field for BNDC in ⟨100⟩-oriented n-type Ge is approximately 2300 V/cm. Referring to the data shown in Fig. 7, one can conclude that when an electric field of 800 V/cm is applied in the minimum mass direction of one or a pair of valleys, an appreciable number of these electrons acquire energies in excess of 0.15 eV, i.e., they transfer to the split-off bands lying 0.15 eV higher in energy. An electric field applied in a ⟨100⟩ direction is less effective in heating the electrons, since their mass is larger than the transverse mass by a factor of $3K/(2K+1)=1.46$, where $K=m_l^*/m_t^*=19.07$. The rate at which electrons absorb energy from an electric field is given by $\mathbf{F}\cdot\boldsymbol{\mu}_\nu\cdot\mathbf{F}$, which is approximately proportional to $\mathbf{F}\cdot(1/\mathbf{m}^*)^\nu\cdot\mathbf{F}$. (Here we are ignoring the anisotropy of the scattering probability, which is small in the present context.) Therefore, for a field in a ⟨100⟩ direction to cause the same amount of heating as a given transverse field, it must be larger in magnitude by a factor of $[3K/(2K+1)]^{1/2}$ than the equivalent transverse field. Thus, in a ⟨100⟩ field of the order of $800\times(1.46)^{1/2}\approx970$ V/cm, a significant number of electrons can be expected to have energies in excess of 0.15 eV. Thus, at a field of 2300 V/cm, the threshold for the BNDC effect in ⟨100⟩ Ge at 77°K, an appreciable fraction of the electrons must have sufficient energy to interact with the ⟨100⟩ Si-like minima.

C. n-Type Silicon

The six lowest conduction-band minima in Si lie along ⟨100⟩ directions in k space and have a mass anisotropy $K=4.8$.[13] We have looked for BNDC effects in n-type Si with the current in the [100] direction and the stress oriented along either [010] or [011]. [010] stress splits the ⟨100⟩ minima into two low-energy valleys with the current along a transverse mass direction, and four high-energy valleys, the current being longitudinal with respect to two of these, and transverse with respect to the other two. [011] stress gives four low-energy valleys transverse to the current and two longitudinal high-energy valleys. We observed no instabilities in Si for fields up to 2.5×10^4 V/cm at 77°K. Typical data at 77°K for a sample with [010] stress are shown in Fig. 8. At low applied stress a finite positive slope is observed up to the maximum field. For a stress of 6250 kg/cm², corresponding to a splitting of 0.05 eV, the current density saturates almost exactly above 2.0×10^4 V/cm. In the absence of measurements of a more detailed nature, such as of the electric field distribution, it cannot be determined whether this saturation is due to a weak BNDC effect which produces a nonuniform field distribution, but no current instabilities, or whether the drift velocity in fact saturates. As the stress is increased this saturation becomes less pronounced, and at higher stresses the curve becomes independent of stress. This latter result suggests that for splittings greater than about 0.08 eV transfer to the higher valleys is negligible for fields up to 2.5×10^4 V/cm. Because of the small specific heat of Si at low temperatures, no reliable results were obtained below 77°K.

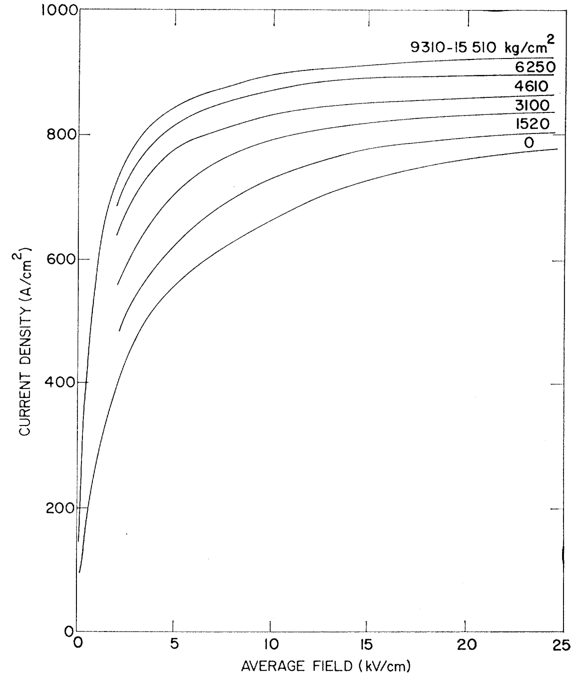

FIG. 8. Current density versus average field for n-type Si with room-temperature resistivity of 8 Ω cm. This data was taken at 77°K and shows almost exact saturation of current density for the intermediate stresses, but no sign of instability.

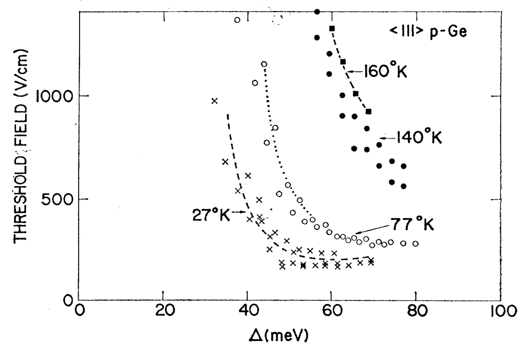

FIG. 9. Threshold field versus valence-band subband edge splitting for p-type Ge. Uniaxial stress and current is along a ⟨111⟩ direction and temperatures are shown in the figure. The material is characterized by room-temperature resistivity of 3 Ω cm and carrier concentration of 1.1×10^{15} cm^{-3}.

[12] A. Jayaraman, B. B. Kosicki, and J. C. Irvin, Phys. Rev. **171**, 836 (1968).

[13] J. C. Hensel, H. Hasegawa, and M. Nakagama, Phys. Rev. **138**, A225 (1963).

D. *p*-Type Ge and InSb

The effect of uniaxial stress on the valence band of Ge-like semiconductors has been discussed in detail by Pikus and Bir.[14] At $k=0$, the effect of compression is to remove the degeneracy of the valence band. For compression along either $\langle 100\rangle$ or $\langle 111\rangle$, the resulting constant-energy surfaces are ellipsoids of revolution, the symmetry axis being the direction of compression. For Ge and InSb, the constant-energy surfaces of the lower-energy valence band are oblate ellipsoids, and those of the higher-energy band are prolate ellipsoids, so that if the electric field is applied parallel to the direction of compression, the longitudinal hole masses are suitably ordered for the occurrence of the Gunn effect. The various masses and splittings for both $\langle 111\rangle$ and $\langle 100\rangle$ stress are listed for both *p*-type Ge and *p*-type InSb in Table II.

Kastal'skii and Ryvkin[4] have reported the existence of Gunn oscillations in uniaxially compressed *p*-type Ge at liquid-helium temperature in lightly doped samples with both $\langle 111\rangle$ and $\langle 100\rangle$ compressive stress. Figure 9 shows the dependence of threshold field on stress at temperatures between 27 and 160°K for $\langle 111\rangle$ stress and current. No oscillations have been observed above 160°K. Even at 27°K, no oscillations were observed for [100] stress. This observation is consistent with the orderings of the effective masses and splittings shown in Table II. In addition, the disappearance of the oscillations above 160°K in $\langle 111\rangle$ samples is consistent with the smaller splitting per unit strain for *p*-type as compared to *n*-type Ge.

[14] G. E. Pikus and G. L. Bir, Fiz. Tverd. Tela **1**, 1642 (1959) [English transl.: Soviet Phys.—Solid State **1**, 1502 (1960)].

As can be seen from Table II, the valence band of InSb has a much larger ratio of longitudinal hole masses under uniaxial compression than does Ge. $\langle 111\rangle$-oriented samples of *p*-type InSb were subjected to uniaxial compressions of up to approximately 9000 kg/cm^2 at 77°K. No evidence of any BNDC effects due to intervalence-band transfer was observed. Instead, above a field of approximately 500 V/cm, the current increased rapidly with time indicating that an increase in current-carrier concentration was taking place. It is believed that the increase is due to excitation of electron-hole pairs by energetic electrons. Although the electron concentration in equilibrium is very low ($\sim 10^5$ cm^{-3}) at low fields at 77°K for the acceptor concentrations used, the generation rate $g(\epsilon)$ for these electrons $[g(\epsilon)\approx n^{-1}(\partial n/\partial t)]$ is expected to be in excess of 10^9 sec^{-1}. Thus, in a few nanoseconds a large portion of the current is carried by electrons. The lack of any strong dependence of the threshold field for this injection effect on applied stress is consistent with the almost complete cancellation of the increase in energy gap due to dilational strain components by the shear-induced valence-band splitting in a $\langle 111\rangle$ direction. The results suggest that for the valence-band splittings attainable ($\lesssim 80$ meV), the heating of the light holes is not sufficient to produce a BNDC even at fields in which the conduction electrons can attain energies of the order of 0.25 eV.

ACKNOWLEDGMENTS

We are grateful to B. L. Crowder for performing the ion implantations. It is a pleasure to acknowledge helpful discussions with W. P. Dumke, J. J. Hall, P. J. Price, and J. F. Woods, and the capable technical assistance of J. A. Bradley, Jr., and F. R. Feigel, Jr.